A physical model for Cenozoic extension of western North America

L.J. Sonder, P.C. England, B.P. Wernicke & R.L. Christiansen

SUMMARY: We investigate the possibility that the onset and development of Cenozoic extension in western North America was governed by the potential energy contrast within, and mechanical properties of, lithosphere that was previously thickened during the Sevier and Laramide Orogenies. The strength of the lithosphere can be defined by its vertically averaged properties; to a first approximation, this strength is too great for geologically significant extension to occur unless the Moho temperature exceeds about 700°C (±100°). This means that there may be a delay between the end of compression and the beginning of extension, the length of which depends on the pre-thickening thermal structure and the compressional strain. Delays of up to 100 My may occur for the lowest initial Moho temperatures investigated (<450°C), or extension may follow immediately on release of compression if the initial Moho temperature exceeds about 700°C. The total extensional strain that is achieved depends on the potential-energy contrast between the thickened lithosphere and its surroundings. Partial melting of peridotite to produce basaltic magma is possible after small degrees of extension, but depends strongly on details of the initial temperature condition in the lower part of the lithosphere.

The results of these calculations agree with observations of the Cenozoic extensional history of North America: late-Mesozoic/early-Tertiary compression in the Pacific Northwest was accompanied by extensive calc-alkaline magmatic activity and was followed almost immediately by extension; in the northern and southern Great Basin—which show respectively, little and no evidence of syn-compressional igneous activity—the gap between compression and extension was 20–40 Ma (N) to about 70 Ma (S).

A number of explanations have been proposed for the Cenozoic extension in western North America. One view relates it to Pacific–Farallon–North American Plate interactions; for example, following Atwater (1970), the extension has often been ascribed to distributed shear resulting from transform motion along the North American Plate boundary. However, this is not easy to reconcile with the fact that the tectonic regime along western North America has been compressive to transpressive through much of the Cenozoic (see data summarized by Wernicke *et al.* this issue), and many details of geography and timing of extension are difficult to relate to any obvious features of Pacific or North American Plate motions. Other explanations rely on inherently untestable assumptions about the mantle underneath North America in the early Tertiary, such as the existence of hot-spots or buoyant subducted slabs.

By contrast, we use a simple quantitative model to consider the hypothesis that extension in the western Cordillera resulted not from forces acting on the base or edges of the North American Plate but from forces in the plate interior inherited from its pre-extensional tectonic history. Much of western North America experienced multiple episodes of compression and crustal thickening during the Mesozoic and earliest Cenozoic eras, and the subsequent extension occurred mainly in a N–S band that coincides with the locus of crustal thickening during the Sevier and Laramide Orogenies (Christiansen & Lipman 1972; Molnar & Chen 1983).

It has long been recognized (e.g. Love 1911; Jeffreys 1929) that regions of isostatically compensated thickened crust may be in a state of extensional deviatoric stress and this has provided the basis for many mechanical explanations of continental extension (e.g. Bott & Dean 1972; McKenzie 1972; Artyushkov 1973; Le Pichon 1982). Molnar & Chen (1983) suggest that extension of the Basin and Range Province resulted from such stresses in a manner analogous to, but more complete than, the present extension of the Tibetan Plateau.

Much of the published work on this topic has concentrated on the existence of potential energy contrasts that create a tendency for thickened crust to extend. Whether or not this tendency results in an appreciable extensional strain rate depends on the instantaneous strength of the lithosphere (a term to be defined later), and the degree of extension depends on the evolution of the potential energy and strength of the lithosphere during stretching. In

From COWARD, M.P., DEWEY, J.F. & HANCOCK, P.L. (eds), 1987, *Continental Extensional Tectonics*, Geological Society Special Publication No. 28, pp. 187–201.

this paper we use a simple mechanical model for the continental lithosphere to calculate the evolution of the strength and potential energy of the lithosphere during compressional and extensional strain. The amount of compressional strain experienced by the continental lithosphere and its post-compressional thermal profile largely determine the amount and timing of its subsequent extension. We investigate the dependence of the total extensional strain and the time of onset of extension on these parameters and attempt an interpretation of the variations in Cenozoic extensional history of western North America in terms of the results of these calculations. This analysis does not preclude contributions from other mechanisms to Cordilleran extension, but it does provide a coherent and testable basis for understanding the origin and timing of Cenozoic extension and related magmatism in western North America.

Evolution of lithospheric strength

To calculate the finite strain of the continental lithosphere we need to calculate strain rates at all points within it. In general this is a formidable problem, but a reasonable first approach is to neglect the (in any case ill-defined) effects of lateral variations in strain and consider the thermal and mechanical evolution of a single column of lithosphere that strains in the vertical and one horizontal direction in response to the potential energy contrast between itself and a reference column of continental lithosphere (see Fig. 3). In addition, we follow previous workers (Bird & Piper 1980; Bird & Baumgardner 1984; England & McKenzie 1982, 1983; England & Houseman 1986; Houseman & England 1986a; Sonder *et al.* 1986; Vilotte *et al.* 1982) and treat the lithosphere as an incompressible thin sheet overlying an inviscid substrate; only vertical integrals of stress and strain rate are considered.

Under these conditions, the strength of the lithosphere may be defined as the vertical integral of the deviatoric stress that is required to produce a given horizontal strain rate. This depends principally on the mineralogy of the rocks that make up the lithosphere, and on their temperatures.

For the purposes of these calculations we adopt the rheology for the continental lithosphere suggested by Brace & Kohlstedt (1980), which contains a brittle upper crust obeying Byerlee's law, a ductile lower crust, the deformation of which is governed by the power-law creep of quartz and a mantle, the deformation of which is governed by Byerlee's law, by high stress plasticity, or by power-law creep of olivine, depending on the strain rate, confining pressure, and temperature. The uncertainty in temperature attached to using these flow laws is discussed below.

Dependence of lithospheric strength on geotherm

Sonder & England (1986) show that for a wide choice of geothermal gradients, the vertically integrated strength of such a lithosphere depends primarily on the temperature at the Moho and on the stress difference at the brittle–ductile transition. This is illustrated in Fig. 1, which shows the dependence of the extensional strain rate on the Moho temperature and on the frictional (Byerlee's law) contribution to the strength for a fixed vertically integrated driving stress of 5×10^{12} N m^{-1}.

The primary geological application of this paper is the extension in the Cordillera of western North America; this has accomplished several tens of percent strain in 30 Ma, thus a relevant strain rate for this problem is a few

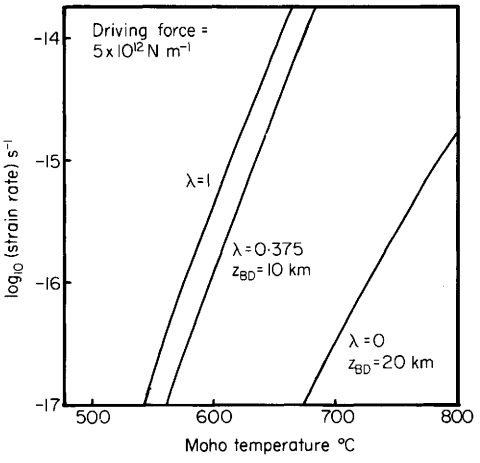

FIG. 1. Extensional strain rate resulting from a driving force of 5×10^{12} N m^{-1} acting on a thin sheet with a vertically averaged rheology containing friction on faults (Byerlee's law), power-law creep of quartz, and Dorn law creep and power-law creep of olivine (see Brace & Kohlstedt 1980). λ is the ratio of pore-fluid pressure to lithostatic pressure in the crust and z_{BD} is the depth to the brittle–ductile transition; when $\lambda = 1$ the deformation is controlled by creep in the upper mantle. Decreasing λ and increasing z_{BD} represent increasing contributions to the strength from friction on faults (see Sonder & England 1986).

times 10^{-16} sec^{-1}. In the cases illustrated in Fig. 1, this strain rate is reached at Moho temperatures between 550 and 750°C. This result is not strongly dependent upon the value of the driving force used and leads us to consider next a simple estimate of the length of time required for the lithosphere to be capable of straining at a geologically significant rate. Figure 1 shows that if a Moho temperature of 750° has been reached, a strain rate of at least 10^{-16} sec^{-1} is calculated for any of the conditions considered.

We assume an initial condition in which shortening is accomplished by uniformly thickening the lithosphere by a factor, f, so that the temperature at a depth, z, is equal to the pre-shortening temperature at depth z/f. We use the method of England & Thompson (1984, appendix B, equation B12) to calculate the approximate amount of time for the Moho to reach 750°C, as a function of the initial Moho temperature and the vertical compressional strain, f.

Figure 2 shows the results of this calculation, using the parameter values listed in Table 1; different initial Moho temperatures correspond to different steady-state mantle heat fluxes. The time required to reach 750°C decreases with the compressional strain and with the initial Moho temperature. Initially hot lithosphere (that had, for example, experienced continental arc volcanism during the compressional stage) could be capable of extending immediately after crustal shortening ends. Conversely, cold lithosphere may take some tens of millions of years to become weak enough to deform. If the amount of thickening is too small, lithosphere may remain cold and strong enough to support the extensional stresses without appreciable extensional strain. Figure 2 indicates that if the compressional strain, f, is less than approximately 1.25, extension will not begin in less than 60–100 My after the end of compression unless the initial Moho temperature is greater than 650°C. Under these circumstances erosion is likely to be a more efficient means of reducing the crustal thickness.

Between these extremes lies a range of degrees of thickening and of Moho temperatures that are relevant to many orogenic belts, and this calculation indicates approximately the conditions under which one might expect such a belt to undergo either no post-compressional extension, extension during or immediately after compression, or extension beginning some tens of millions of years after the end of compression. However, this treatment neglects any influence of strain on the geotherm and provides no estimate of the amount of extension. In the following section we describe calculations that have a bearing on the thermal and mechanical evolution of such a lithosphere after extension begins.

A physical model for extension following compression of continental crust

Description of the model

We define a reference state for continental lithosphere by requiring it to be in isostatic and potential energy equilibrium with oceanic lithosphere and in thermal steady-state with basal temperature, T_1, and heat production, H_0, distributed uniformly throughout the crust (see Fig. 3). Instantaneous homogeneous thickening of the reference lithosphere perturbs the geotherm and changes the potential energy of the lithosphere. The contrast in potential energy between the thickened lithosphere and the reference lithosphere gives rise to deviatoric stresses that can drive extension if the strength of the lithosphere permits.

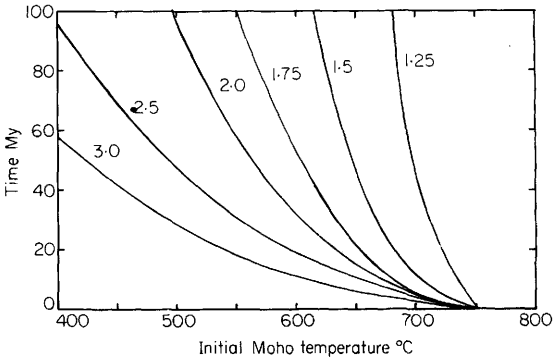

FIG. 2. Time required for the Moho temperature to reach 750°C, as a function of initial Moho temperature and compressional strain f using the method of England & Thompson (1984, appendix B, equation B12). The value of f is indicated beside each curve.

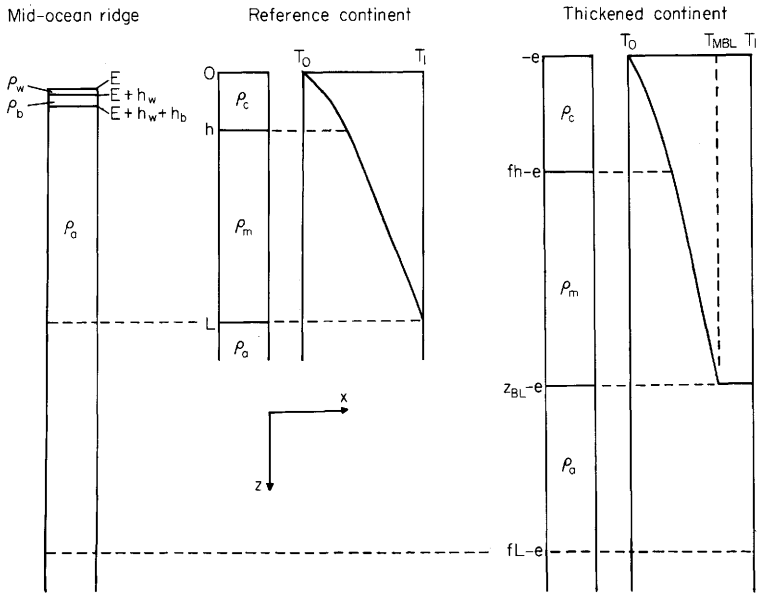

FIG. 3. Reference state and initial density and temperature conditions for the calculations of this paper. Reference lithosphere is in potential energy and isostatic equilibrium with mid-ocean ridge; under these conditions crustal density, ϱ_c, and elevation, E, are constrained once values for crustal thickness, h, and heat production, H_0, are chosen (see Table 1 for parameter values). Reference lithosphere is assumed to be in thermal steady-state with heat production H_0 distributed uniformly throughout the crust, and with surface and basal temperatures T_0 and T_1, respectively. Initial conditions are a consequence of uniformly and instantaneously thickening the reference continent by a factor f. The elevation change associated with isostatic response to the thickening is e. At depth z_{BL}, where the temperature is T_{MBL}, the lower portion of the lithosphere is assumed to detach and be replaced by asthenosphere with temperature T_1 (see text).

The thermal and mechanical evolution of thickened continental lithosphere depends strongly on the choice of a lower boundary condition. Since the lithosphere can be regarded as a mechanically rigid layer overlying a convecting asthenosphere, there must be a thermal boundary layer at the base of the lithosphere across which heat is transferred dominantly by conduction, but which is hotter, hence weaker, than the overlying mechanical lithosphere (see, e.g. Parsons & McKenzie 1978). Houseman *et al.* (1981) have shown that a lithospheric thickening event, such as occurred in the Mesozoic and early Cenozoic in western North America, can result in instability of the thickened thermal boundary layer, which consequently detaches from the mechanical lithosphere and is replaced by material at asthenospheric temperatures. The time at which detachment occurs depends on the intensity of mantle convection and, in the cases illustrated by Houseman *et al.*, lies between 0 and 100 My after the end of thickening.

We assume that during compression of the continent the mechanical lithosphere is thickened to the same extent as the crust; however, we follow Houseman *et al.* (1981) in recognizing the instability of the thickened thermal boundary layer. In the absence of any constraint on the timing of the detachment of the thermal boundary layer, we assume that it occurs at the end of compression. We define the base of the mechanical boundary layer (i.e. the depth at which detachment occurs) by an isotherm, T_{MBL}, which we take to be a free parameter. The exact form of the boundary and initial conditions, and a summary of the governing equations, are contained in the Appendix.

For the rest of this paper, we shall be concerned with the evolution of the potential energy and thermal profile of the lithosphere from these initial conditions, and the resulting strain history. In order to reduce the number of parameters investigated, we neglect the contribution of the crust to the strength of the lithosphere. Thus our results represent the maximum extension to be expected from the model discussed in this paper.

The extensional strain, β, is defined as the ratio of the crustal thickness immediately after the shortening event to its thickness at a subse-

TABLE 1. *Values of parameters used in the calculations.*

L	Reference lithosphere thickness	110 km
h	Reference crustal thickness	33.75 km
h_w	Water depth above mid-ocean ridge	2.5 km
h_b	Crustal thickness at mid-ocean ridge	5.0 km
ϱ_w	Density of water	1.03×10^3 kg m^{-3}
ϱ_b	Density of oceanic crust	2.96×10^3 kg m^{-3}
ϱ_c^0	Density of continental crust at $T=T_0$	2.82×10^3 kg m^{-3}
ϱ_m^0	Density of mantle at $T=T_0$	3.33×10^3 kg m^{-3}
ϱ_a	Density of asthenosphere at $T=T_1$	3.17×10^3 kg m^{-3}
α	Coefficient of thermal expansion	3.4×10^{-5} K^{-1}
C_p	Specific heat	1.2×10^3 J kg^{-1} K^{-1}
κ	Thermal diffusivity	8×10^{-7} m^2 sec^{-1}
K	Thermal conductivity	2.6 W m^{-2} K^{-1}
H_0	Crustal heat production	1.15×10^{-6} W m^{-3}
T_0	Surface temperature	0°C
T_1	Asthensophere temperature	1400°C
T_{MBL}	Temperature at base of mechanical lithosphere	1120°C
g	Gravitational acceleration	9.8 m sec^{-2}
f	Compressional strain	2.0

quent time. The compressional strain, f, is the ratio of the crustal thickness immediately after compression to that of the crust in the reference continent (see Fig. 3).

Two other parameters are of importance in these calculations; they are the immediate post-thickening Moho temperature, $T_M(0)$, and the temperature T_{MBL} that defines the base of the mechanical lithosphere. Each of the values of the parameters in Table 1 is uncertain to ±10% at least, but the results of the calculations are most sensitive to the three parameters f, $T_M(0)$ and T_{MBL}. The values of the parameters used in the calculations are those given in Table 1, except where explicitly stated otherwise. $T_M(0)$ is varied by changing the crustal heat production, H_0.

Timing of extension

Figure 4 shows the evolution over time of the elevation, extensional strain, heat flow, effective viscosity (vertically averaged stress divided by strain rate), strain rate, and Moho temperature for a calculation using the parameter set defined in Table 1. Results can be divided into three phases: pre-extension, syn-extension, and post-extension.

The pre-extension phase lasts approximately 30 Ma and represents the period of time for the geotherm to relax to a stage where the strength of the lithosphere is low enough to permit deformation at an appreciable strain rate. During this time the Moho temperature increases from 600 to almost 700°C (cf. Fig. 2) and the strain rate increases by two orders of magnitude. The initial elevation is slightly over 4 km as a result of isostatic compensation for almost 70 km of crust (compare with Tibet, where the elevation is mainly between 5 and 6 km, and with the Altiplano of western South America, where elevations reach about 4.5 km). Surface heat flow, which immediately after thickening is half that of the reference lithosphere, increases only slightly before major extension starts.

In the succeeding 20 Ma, 90% extension ($\beta=1.9$) occurs, bringing the crustal thickness back almost to its pre-thickening value; the elevation drops sharply in isostatic compensation for the thinning of low-density crust, and the surface heat flux increases rapidly, reflecting the upward transport of hot material as the lithosphere thins. During the early phase of extension the Moho temperature continues to increase, but in the later stages (around 45–50 Ma elapsed time) the Moho temperature begins to fall as the Moho is brought close enough to the surface to begin cooling (see England 1983; Houseman & England 1986b).

Once deformation stops, the elevation subsides slowly as temperatures fall and the average densities of the crust and mantle increase. Because in this example the strain resulting from thickening, f, almost equals the extensional strain, β, the Moho temperature and the surface heat flow return to close to their pre-thickening values after a long time has elapsed.

Figures 5 & 6 show results from calculations starting with thermal profiles that are hotter and colder, respectively, than the initial thermal profile of Fig. 4. If the Moho temperature is suffi-

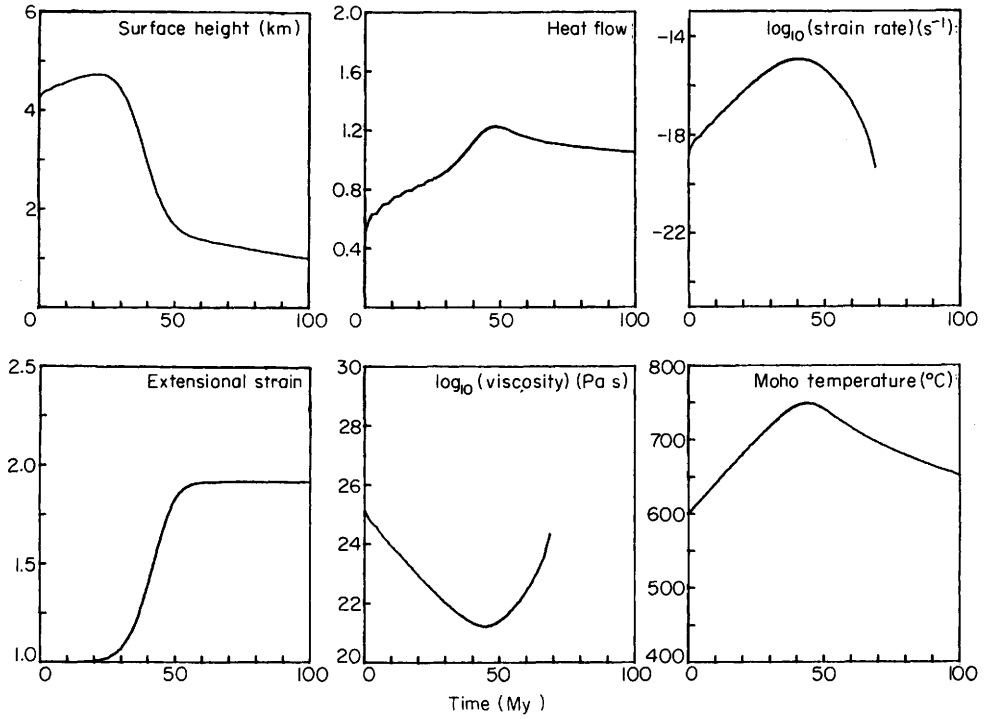

FIG. 4. Elevation, extensional strain (β), surface heat flow, effective viscosity (vertically averaged stress divided by strain rate), strain rate and Moho temperature as functions of time, for a calculation using parameter values listed in Table 1. Heat flow is normalized to that of the reference continent, which for this calculation is 67 mW m^{-2}, and initial Moho temperature, $T_M(0)$ is 600°C. Strain rate and effective viscosity are not plotted after the strain rate falls below 10^{-19} sec^{-1}.

ciently high, extension can begin immediately after shortening ends (see Fig. 2). This is shown in Fig. 5, where the initial Moho temperature is 700°C (other parameter values are as for Fig. 4). The strain rate is almost at its maximum value immediately after compression stops, rises slightly during the first part of the extension, then falls monotonically as the potential-energy contrast, and hence the deviatoric stress, decreases. Deformation has ceased by 25 Ma and results in approximately 110% extensional strain. Accompanying the extension, the elevation falls from almost 3.5 to less than 1 km. Because the deformation occurs rapidly compared with the time needed for the decay of thermal perturbations, temperatures change very little during extension; for example, the Moho temperature varies by less than 100°C.

The evolution of thickened lithosphere with a cold initial thermal structure is shown in Fig. 6. Parameters were chosen to give an initial Moho temperature of 550°C. The effect of such cold temperatures is to inhibit extension until about 50 Ma after the end of compression; however, by this time the Moho temperature has risen close to 700°C (compare Fig. 4) and extension of about 70% is achieved in the next 25 Ma.

Figures 4–6 show that, as suggested by the approximate calculation of Fig. 2, the time at which extension begins depends on the thermal profile at the end of compression. Figure 7 illustrates this by plotting the time at which extensional strain rates exceed 10^{-16} sec^{-1} for a wider range of the parameters $T_M(0)$, f and T_{MBL}.

The curves of Figs 2 & 7 are qualitatively similar, and this suggests that the time interval required for the Moho temperature to reach 750°C (Fig. 2) is a useful approximation of the time required for extension to begin. There are quantitative differences between Figs 2 & 7, which result from the fact that in Fig. 7 the criterion for the onset of extension is strain rate, not Moho temperature, so that differences in the initial potential energy of the column influence the time at which the specified strain rate (10^{-16} sec^{-1}) is reached. The potential energy contrast is determined largely by the amount of compressional strain, f, and by the amount of lithosphere that detaches immediately after compression (see above). For Fig. 7(a), no

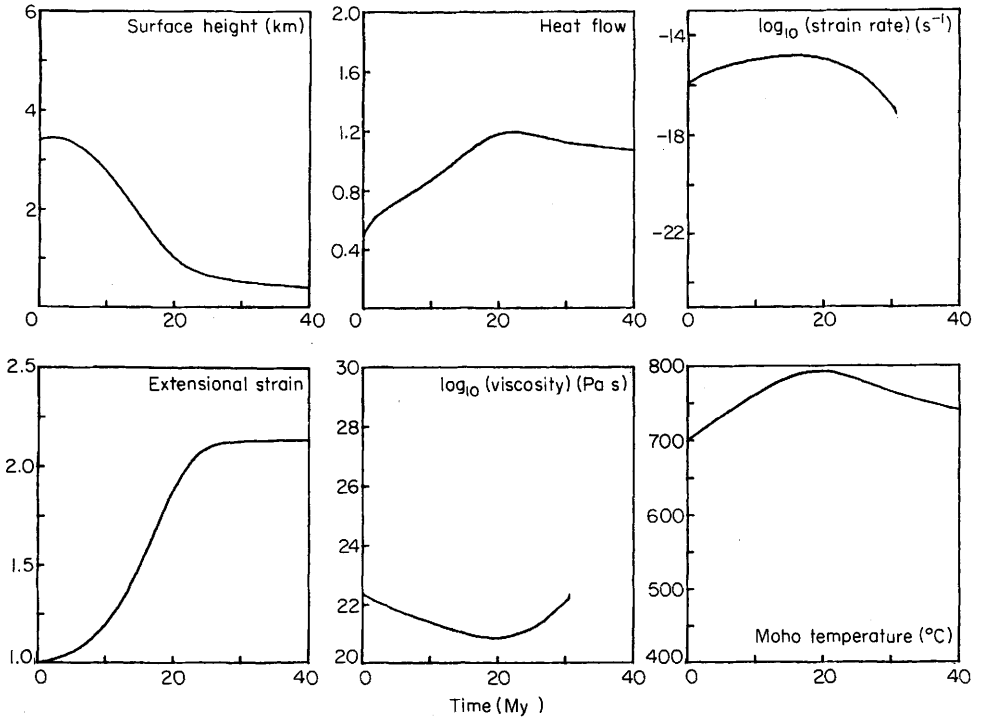

FIG. 5. Similar to Fig. 4, but with $H_0 = 1.9 \times 10^{-6}$ W m^{-3}, $T_M(0) = 700$°C. Heat flow is normalized to 88 mW m^{-2}.

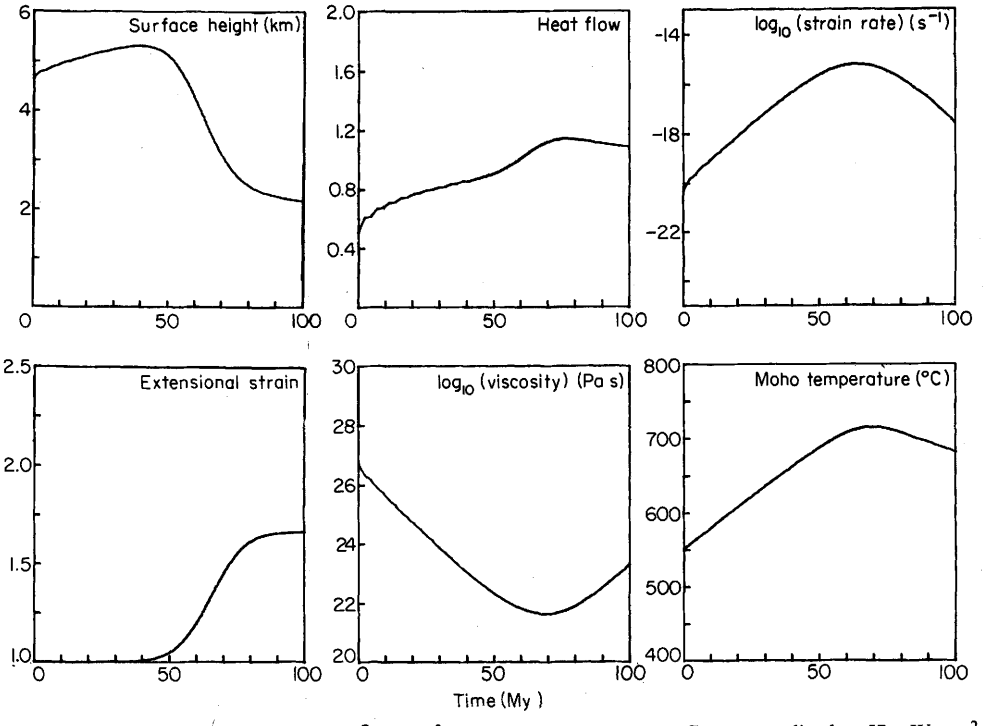

FIG. 6. As Fig. 4, but with $H_0 = 8.2 \times 10^{-7}$ W m^{-3}, $T_M(0) = 550$°C, and heat flow normalized to 57 mW m^{-2}.

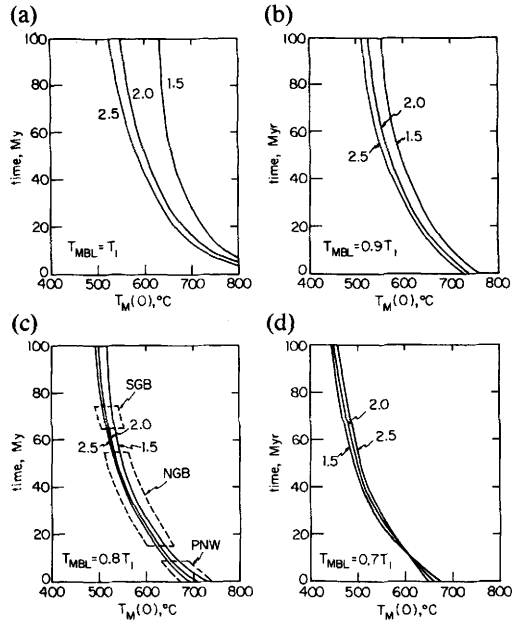

FIG. 7. Time required for extensional strain rate to reach 10^{-16} for calculations using the values of parameters given in Table 1, except that the initial Moho temperature, $T_M(0)$ is varied between 400 and 800°C by adjusting H_0, and T_{MBL} is varied from T_l to $0.7 \times T_l$. Curves are shown for $f = 2.5$, 2 and 1.5. Boxes labelled PNW, NGB and SGB show the ranges of time and $T_M(0)$ for the Pacific Northwest, northern Great Basin and the 'amagmatic corridor' in the southern Great Basin.

lithosphere detaches, and curves differ from their counterparts in Fig. 2 mainly because of the variation in the initial potential energy contrasts. Figure 7(b), (c) and (d) represent cases in which detachment of a portion of the lithosphere occurs; this strongly affects the potential energy of the lithosphere column, and the time at which extension begins. When approximately 20% or more of the lithosphere is detached (i.e. $T_{MBL} \leq 0.8\ T_l$) the influence of this upon the potential energy is much greater than the effect of variations in compressional strain, so that there is a difference of less than 5 Ma in the time of onset of extension for different values of f (Fig. 7c & d).

Amount of extension

We have seen that the time required for extension to begin is strongly dependent upon the initial potential energy excess of the thickened lithosphere. If thermal diffusion were unimportant the same quantity would determine the *total* strain which the column of lithosphere could undergo. However, thermal diffusion influences the maximum extension in two ways: it affects the strength of the lithosphere, and it acts to change the density of the lithosphere, and hence its potential energy excess. Therefore, the total amount of extension that can be achieved depends not only upon the initial temperature and density structure, but upon the thermal and mechanical evolution through time. There is no simple relationship between the maximum extensional strain and the thermal state of the lithosphere at the end of compression, but Fig. 8 shows the results of our calculations.

The maximum extensional strain increases with the initial potential energy excess—that is, with increasing crustal compressional strain or decreasing thickness of the mechanical boundary layer (i.e. decreasing T_{MBL}). The extensional strain decreases with lower initial Moho temperature, and this is mainly the result of the higher strength of cold lithosphere, which inhibits deformation even when the potential energy contrast is non-zero. (Lowering the Moho temperature also has the effect of slightly lowering the potential energy of the lithosphere, but this is a relatively unimportant factor.)

Figure 8 also indicates that there is a range of conditions in which the maximum extensional strain exceeds the compressional strain, resulting in a final crustal thickness less than that of the reference lithosphere.

Discussion

The model for extension of over-thickened continental lithosphere that we have presented in this paper depends only upon the observation that the potential energy stored during the thickening of continental crust will tend to be released by the extension of the thickened crust once the compressive stress required for orogeny

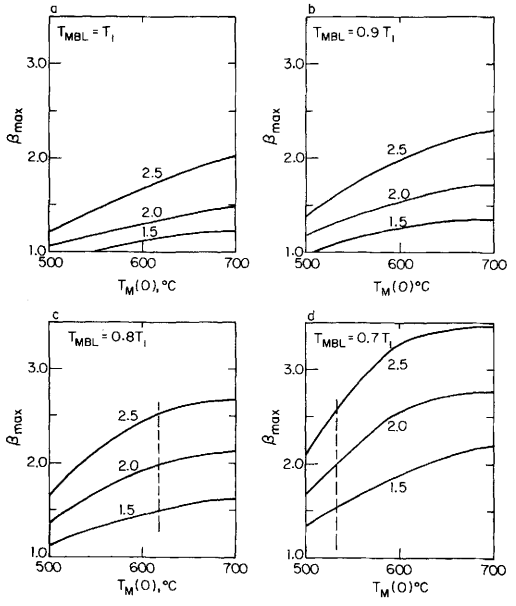

FIG. 8. Maximum extension, β_{max}, as a function of T_{MBL}, $T_M(0)$ and f. Other parameters as in Table 1. The dashed lines in (c) and (d) separate conditions for which $\beta_{max} > f$ from those in which $\beta_{max} < f$.

is removed (e.g. Molnar & Lyon-Caen in prep.). The purpose of this section is to investigate to what extent the Tertiary extensional history of western North America may be explained by such a model, and to see what features of that history demand the action of forces other than those arising from the late-Mesozoic crustal thickening which is known to have affected the region.

The extensional history calculated from the model presented above depends strongly upon two parameters—the Moho temperature and the excess potential energy of the lithospheric column immediately after the thickening episode. Neither of these parameters is well constrained by geological observations that we can make on the region 50 Ma or more after the end of compression. However, the calculations of Fig. 7 show that the inverse dependence on the initial Moho temperature, $T_M(0)$, of the time interval between the end of compression and the onset of extension is preserved almost independently of the initial potential energy excess. Consequently, if this model is relevant to the Tertiary history of western North America, we should expect a similar dependence of this time interval on Moho temperature. Although it is not possible to estimate absolute values of Moho temperature, observations summarized by Wernicke *et al.* (this issue) indicate that the relative timing of extension in three separate parts of the North American Cordillera is consistent with our calculations.

Relative timing of extension in the Pacific Northwest, and northern and southern Great Basin

Wernicke *et al.* (this issue, table 1) summarize the time intervals between the end of major compression and the onset of extension in these three regions. In the Pacific Northwest the latest major compressional event appears to have been no older than 58 Ma, and the onset of extension was no later than about 49 Ma, an interval of approximately 9 Ma. In the northern Great Basin, the equivalent interval was from mid-Eocene to early Miocene; although there was localized extension between 10 and 20 Ma after the end of thickening, the major extension occurred between 20 and 40 Ma after the end of compression. In the southern Great Basin, this interval is even longer, extending from 90 to 20 Ma.

An indication of the relative Moho temperatures in these terrains may be obtained from their pre-extensional tectonic histories. In the Pacific Northwest, extensive calc-alkaline plutonism and volcanism accompanied the crustal thickening, and it seems reasonable to assume high sub-Moho temperatures in this region at the end of shortening; indeed, the extensive calc-alkaline activity suggests that much of the lower crust may have been partially molten. In contrast, the northern Great Basin experienced only minor amounts of igneous activity towards the end of its Mesozoic compressional history, as would be consistent with the

thickening of continental crust of average geothermal gradient (see, e.g. England & Thompson 1984, in press). The 'amagmatic corridor' in the southern Great Basin exhibited no magmatic activity during this time.

Figure 7(c) shows the lengths of the time intervals between compression and extension in these three regions, and indicates the approximate post-compressional Moho temperatures required if the model calculations are to yield the same time interval. The 65–75 Ma interval of the southern Great Basin would require Moho temperatures of 500–550°C, the 15–55 Ma of the northern Great Basin would require Moho temperatures of 525–650°C, and Moho temperatures in the range 625–725°C would give the interval of 20 Ma or shorter shown in the Pacific Northwest. These relative Moho temperatures are consistent with the late-Mesozoic/early-Cenozoic history of these regions but, of course, no absolute Moho temperatures can be determined. Although, as discussed below, there is an uncertainty, due to extrapolating laboratory flow laws, of ±100°C in the absolute values of temperatures shown in Figs 4–8, this does not affect the relative temperatures we discuss.

Magmatic activity

As discussed in our companion paper, the Tertiary extensional and magmatic histories of western North America are closely interlinked. Owing to three sources of uncertainty, it is impossible to make a quantitative calculation of the volume or chemistry of the magmas that would result from the thermal histories we discuss above. First, without a knowledge of the rates of ascent of various magma types through the lithosphere, the geothermal regimes that we calculate are schematic if a large proportion of the heat is carried by magma. Secondly, although we may calculate conductive temperature regimes and relate them to choices of solidus, we calculate strain histories by extrapolating laboratory flow laws over approximately six orders of magnitude in strain rate. There is an uncertainty of at least 100°C attached to this extrapolation if we wish to determine the temperatures at which the lithosphere will deform at a given strain rate; consequently a region that is characterized by a given strain history may well have experienced that strain under a regime where the Moho temperature was 100°C higher than would be calculated using the values of laboratory flow-law parameters listed in Table 1. Finally, the chemistry of magma that reaches the surface depends critically upon the composition of the lower crust and the time available for fractionation and mixing during the ascent of the magma through the lithosphere.

Extension of continental lithosphere of normal thickness is almost certain to result in basaltic magmatism as uppermost asthenosphere—initially close to the solidus—is decompressed nearly adiabatically (e.g. Beaumont *et al.* 1982). In the cases described here, the immediately post-compressional lithosphere is far thicker than normal, although its thickness is reduced by instability of the thermal boundary layer; diffusion of heat may also considerably raise the temperature of the lower lithosphere before extension begins.

Figures 9 & 10 compare the geotherms before and during extension with estimated crust and mantle solidi for calculations with two different sets of parameters.

In the case illustrated in Fig. 9, the isotherm defining the base of the mechanical lithosphere is taken to be 1000°C, and the bottom 70 km—the thermal boundary layer—of the thickened lithosphere is replaced by asthenosphere immediately after the compressional episode. The choice of asthenospheric temperature in this calculation is such that a small portion of the lowermost lithosphere is above the peridotite solidus even before extension begins at about 30 Ma. During extension, much more of the lithosphere passes above the peridotite solidus until at 43 Ma (the end of extension) the geotherm intersects the solidus at 70 km. In Fig. 10 the isotherm defining the base of the mechanical lithosphere is taken to be 1150°C, and the geotherm does not pass above the peridotite solidus until half the extension is accomplished, and even at maximum extension, the geotherm does not lie much above the solidus.

The generation of basaltic melt during extension thus depends on an indeterminate quantity: the ratio of the temperature at the base of the lithosphere at the onset of extension to the mantle solidus temperature at that depth. However, the observation that basaltic volcanism almost invariably post-dates the onset of extension in western North America (Wernicke *et al.* this issue) is in agreement with the model proposed here, provided that the lowermost 20–30% of the lithosphere is unstable in the fashion suggested above. The left-hand sides of Figs 9(a) & 10(a) show the relationships of the geotherms in the crust to various solidi for crustal materials; in each case the thermal relaxation before extension begins has been sufficient to raise the lowermost 5–15 km of the crust

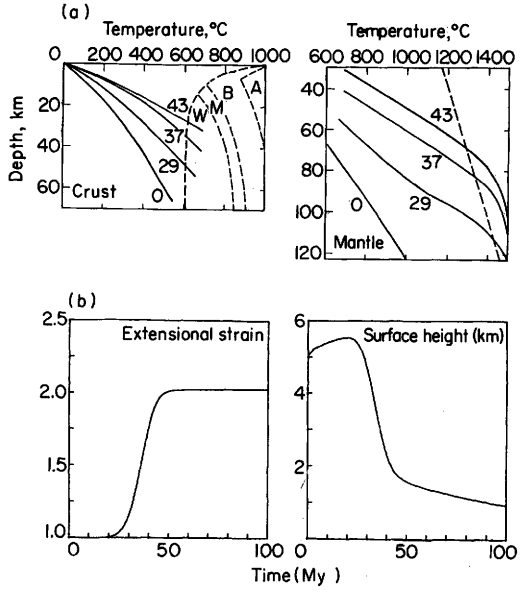

FIG. 9. (a) Geotherms at selected times for calculations illustrated in (b). Times in Ma are shown beside each curve. Geotherms are split at the Moho into crust and mantle portions and are plotted separately. Dashed lines indicate solidi appropriate to reasonable compositions of crust and mantle rocks: for the crust we show curves from Wyllie (1977) for water-saturated melting (W), and melting in the presence of muscovite and biotite in metapelites and peraluminous granites (M), biotite and hornblende in granodiorite–tonalite (B), and hornblende in amphibolites (A). For the mantle we have plotted a dry peridotite solidus from Kushiro *et al.* (1972). (b) Surface elevation and extension as a function of time for a calculation with the parameters given in Table 1, except that $T_1 = 1500°C$, $H_0 = 5.9 \times 10^{-7}$ W m^{-3}, $T_M(0) = 550°C$, $T_{MBL} = 1000°C$ and $f = 1.75$. Heat flow is normalized to 52 mW m^{-2}. Calculated geotherms for these conditions are shown in (a).

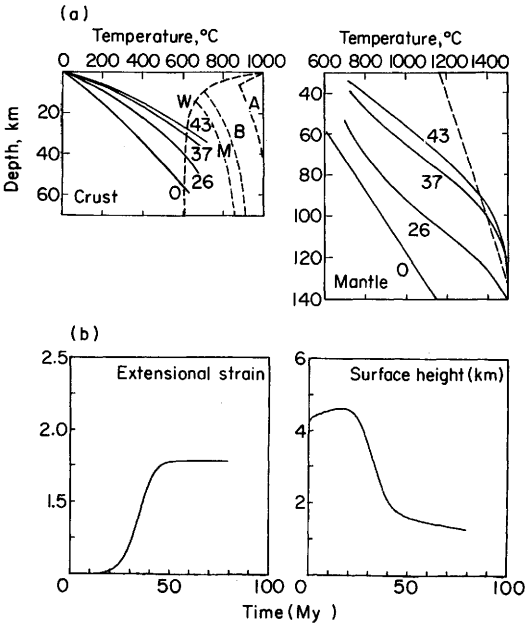

FIG. 10. As Fig. 9, except that $T_{MBL} = 1150°C$ and $H_0 = 1.0 \times 10^{-6}$ W m^{-3}, $T_M(0) = 630°C$, and heat flow is normalized to 64 mW m^{-2}. Initial Moho temperature has been adjusted to give total extension comparable with the calculation in Fig. 9.

above a temperature of 600°C. We emphasize again the uncertainty of ±100°C in the absolute values of these temperatures, but suggest that the syn-extensional bimodal magmatism in the Great Basin may be explained by the interaction of basaltic melt, produced in an adiabatically decompression upper mantle, with a lower crust that has been heated by thermal relaxation of the thickened lithosphere.

Comparison with the present Basin and Range Province

Figures 4–6 illustrate *possible* thermal and mechanical histories of the Pacific Northwest (Fig. 5), northern (Fig. 4) and southern (Fig. 6) Great Basin. We do not wish to imply that they represent the only conditions under which such extension could occur: Figs 7 & 8 show that

several other parameter combinations would produce similar results.

Here we compare the results of two calculations with observations of the crustal thickness, elevation, heat flow, seismic lithosphere thickness, and strain rate in the Great Basin. The calculations are those of Figs 4 & 9; each has an interval of 20–30 My between compression and extension and the calculations differ in that the initial conditions for Fig. 9 involved less crustal thickening, a lower Moho temperature and thinner lithosphere than for Fig. 4.

Crustal thickness in the Great Basin is between 25 and 30 km (Smith 1978); the elevation in the Great Basin is between 1.5 and 2 km (Eaton *et al.* 1978) and the average elevation of Nevada N of 38°N is 1.8 km (Navy Fleet Numerical Oceanography Center 1982); the average heat flow in the Basin and Range is 90 mW m^{-2} (Lachenbruch & Sass 1978); the depth to the top of the low-velocity zone for shear waves is about 65 km (Burdick & Helmberger 1978; Priestley *et al.* 1980). The present strain rate in the Basin and Range is poorly constrained; Minster & Jordan (1984) place an upper limit of 8 mm yr^{-1} on the extension of North America E of the San Andreas system and Smith (this issue) estimates extension rates of between 1 and 20 mm yr^{-1} within the Basin and Range. Divided by a width of 700 km for the province these estimates amount to strain rates of 3.5×10^{-16} sec^{-1} and 4.5×10^{-17} sec^{-1} to 9×10^{-16} sec^{-1} respectively.

Table 2 lists these estimates and compares them with the quantities calculated for Figs 4 & 9. It is not possible to quantify the uncertainty involved in comparing an estimate of lithospheric thickness based on calculated geotherms with an estimate based on the depth of the top of a shear-wave low-velocity zone. The only quantitative disagreement between the calculations and the observations is in the crustal thickness for Fig. 4; this figure could doubtless be adjusted, but it would serve no useful purpose, as better agreement may be obtained by adjusting one or more of the initial conditions (e.g. as has been done for Fig. 9), none of which is well constrained by observation.

Conclusions

The geological observations reviewed by Wernicke *et al.* (this issue) indicate that Cenozoic extension in western North America is not related in a simple way to plate-boundary forces; for much of the time that extension was operating in the continental interior, the strain on the western margin of North America was compressive or transpressive. This, together

TABLE 2. *Comparison between calculated and observed values of crustal thickness elevation, heat flow, lithsophere thickness and strain rate.*

	Great Basin[1]	Fig. 4[2]	Fig. 9[3]
Crustal thickness	25–30 km	37 km	31 km
Original crustal thickness[4]	—	33.75/67.5 km	33.75/59.1 km
Elevation	1.5–2 km, 1.8 km	1.7 km	1.7 km
Original elevation[5]	—	0.2 km	0.2 km
Heat flow	90 (±30) mW m^{-2}	80 mW m^{-2}	70 mW m^{-2}
Original heat flow[5]	—	65 mW m^{-2}	52 mW m^{-2}
Seismic lithospheric thickness	65 km	—[6](90 km)	70 km[6] (60 km)
Strain rate	$<3.5 \times 10^{-16}$ sec^{-1} 4.5×10^{-17} – 9×10^{-16} sec^{-1}	4.5×10^{-16} sec^{-1}	5×10^{-16} sec^{-1}

[1]See text for sources.
[2]Parameter values given in caption to Fig. 4 and Table 1. Time after end of thickening, 50 Ma; $\beta = 1.8$.
[3]Parameter values given in caption to Fig. 9 and Table 1. Time after end of thickening, 43 Ma; $\beta = 1.9$.
[4]First value, crustal thickness before compression; second value, crustal thickness immediately after compression.
[5]Values before compression.
[6]Depth to intersection of geotherm with peridotite solidus that is used in Figs 9 & 10. Numbers in parentheses indicate values obtained by taking depth at which geotherm reaches 100°C less than the solidus temperature.

with the observation that the locus of extension correspond to the locus of Mesozoic crustal thickening (e.g. Coney & Harms 1984), lends support to the suggestion that the buoyancy force associated with crustal thickening may have had a major influence on subsequent extensional tectonics of the region (e.g. McKenzie 1972; Molnar & Tapponnier 1978; Molnar & Chen 1983). However, the onset of extension in the Cordillera did not follow directly, nor indeed at any constant interval, after the end of compression. While a state of extensional deviatoric stress may have existed throughout much of the Cenozoic in this region, it was not expressed in appreciable extensional strain for a time that varied from less than 10 My in the Pacific Northwest to over 70 My in the southern Great Basin.

The physical model presented in this paper treats the continental lithosphere in terms of the vertical averages of its rheology and of the stresses acting upon it. The rheology is based on laboratory flow laws (see Description of Model, and Brace & Kohlstedt (1980)), and the stresses acting upon the lithosphere are solely those that arise from changing its thickness and thermal structure while maintaining isostatic balance with a reference continental column.

If such a continental lithosphere is thickened it is gravitationally unstable and will tend to spread under its own weight. The strength of the rheologically stratified lithosphere depends on its thermal regime, which may conveniently be characterized by the Moho temperature (Sonder & England 1986). Over the range of conditions discussed here, the deviatoric stresses associated with thickened lithosphere do not result in appreciable extensional strain until the Moho temperature is greater than about 700°C (see, e.g. Figs 4, 5 & 6). Consequently, there is a time interval between the end of compression and the onset of extension that depends on the time required for thermal relaxation to warm the lithosphere and, to a lesser extent, on the excess potential energy stored in the thickened lithosphere (see Fig. 7). For the lowest initial Moho temperatures considered (<450°C) this length of time exceeds 100 My, and it is likely that erosion, rather than extension, would reduce the thickness of such a mountain belt. However, for initial Moho temperatures between 500 and 700°C, the time interval drops from around 100 Ma to zero (Fig. 7). In the calculations illustrated in Fig. 8, extension occurs until the lithosphere is in potential energy balance with the reference continental column, and in many cases (see Fig. 8c & d) the total extension may exceed the original compressional strain, leaving crust thinner than before compressional strain began. Under these conditions, the lithosphere is substantially thinner at the end of extension than it was originally, and it is likely that basaltic melts are produced by adiabatic decompression of the asthenosphere during extension; the intrusion of such melts into lower crust already close to its solidus could well result in bimodal magmatism during the extension.

The predominant testable feature of the physical model presented here is the inverse dependence of the time interval between compression and extension on the Moho temperature at the end of compression. Insofar as thermal regimes may be estimated from syn-compressional magmatic activity, this is a feature that is shared by the Cenozoic extensional terrains of western North America (see above and Wernicke *et al.*, this volume).

ACKNOWLEDGMENTS: It is a pleasure to acknowledge the countless conversations and arguments with Peter Molnar that have raised the level of our understanding of the mechanics of mountain belts. This work was made much easier by Greg Houseman's generous help in writing the computer programs. We were supported by NSF grants EAR84-08352 and EAR83-19767. L.J.S. acknowledges support from an Exxon Teaching Fellowship.

References

ARTYUSHKOV, E.V. 1983. Stresses in the lithosphere caused by crustal thickness inhomogeneities. *J. geophys. Res.* **78**, 7675–708.

ATWATER, T. 1970. Implications of plate tectonics for the Cenozoic tectonic evolution of western North America. *Bull. geol. Soc. Am.* **81**, 3513–36.

BEAUMONT, C., KEEN, C.E. & BOUTILIER, R. 1982. On the evolution of rifted continental margins: comparision of models and observations for the Nova Scotian margin. *Geophys. J. R. astron. Soc.* **70**, 667–715.

BIRD, P. & BAUMGARDNER, J. 1984. Fault friction, regional stress, and crust–mantle coupling in southern California from finite element models. *J. geophys. Res.* **89**, 1932–44.

—— & PIPER, K. 1980. Plane-stress finite-element models of tectonic flow in southern California. *Phys. Earth planet. Inter.* **21**, 158–75.

BOTT, M.H.P. & DEAN, D.S. 1972. Stress systems at young continental margins. *Nature*, **235**, 23–5.

BRACE, W.F. & KOHLSTEDT, D.L. 1980. Limits on lithospheric stress imposed by laboratory experiments. *J. geophys. Res.* **85**, 6248–52.

BURDICK, L.J. & HELMBERGER, D.V. 1978. The upper mantle *P* velocity structure of the western United States *J. geophys. Res.* **83**, 1699–712.

CHRISTIANSEN, R.L. & LIPMAN, P.W. 1972. Cenozoic volcanism and plate tectonic evolution of the western United States II. Late Cenozoic. *In*: *A Discussion on Volcanism and the Structure of the Earth, Phil. Trans. R. Soc. London*, **A217**, 249–84.

CONEY, P.J. & HARMS, T.A. 1984. Cordilleran metamorphic core complexes: Cenozoic extensional relics of Mesozoic compression. *Geology*, **12**, 550–4.

EATON, G.P., WAHL, R.R., PROSTKA, H.J., MAHEY, D.R. & KLEINKOPF, M.D. 1978. Regional gravity and tectonic patterns: Their relation to late Cenozoic epeirogeny and lateral spreading in the western Cordillera. *In*: SMITH, R.B. & EATON, G.P. (eds) *Cenozoic Tectonics and Regional Geophysics of the Western Cordillera. Mem. geol. Soc. Am.* **152**, 51–91.

ENGLAND, P.C. 1983. Constraints on extension of continental lithosphere. *J. geophys. Res.* **88**, 1145–52.

—— & HOUSEMAN, G.A. 1986. Finite strain calculations of continental deformation II. Comparison with the India–Asia collision. *J. geophys. Res.* **91**, 3664–76.

—— & MCKENZIE, D.P. 1982. A thin viscous sheet model for continental deformation. *Geophys. J.R. astron. Soc.* **70**, 295–321.

—— &—— 1983. Correction to: A thin viscous sheet model for continental deformation. *Geophys. J.R. astron. Soc.* **73**, 523–32.

—— & THOMPSON. A.B. 1984. Pressure–temperature–time paths of regional metamorphism I. Heat transfer during the evolution of regions of thickened continental crust. *J. Petrol.* **25**, 894–928.

—— &—— In press. Some thermal and tectonic models for crustal melting in continental collision zones. *J. geol. Soc. London.*

HOUSEMAN, G.A. & ENGLAND, P.C. 1986a. A dynamical model for lithosphere extension and sedimentary basin formation. *J. geophys. Res.* **91**, 719–29.

—— & —— 1986b. Finite strain calculations of continental deformation I. Method and general results for convergent zones. *J. geophys. Res.* **91**, 3651–63.

—— , MCKENZIE, D.P. & MOLNAR, P. 1981. Convective instability of a thickened boundary layer and its relevance for the thermal evolution of continental convergent belts. *J. geophys. Res.* **86**, 6115–32.

JEFFREYS, H. 1929. *The Earth*, 346 pp. Cambridge University Press, Cambridge, England.

KUSHIRO, I., SHIMIZU, N. & NAKAMURA, Y. 1972. Compositions of coexisting liquid and solid phases formed upon melting of natural garnet and spinel lherzolites at high pressures: a preliminary report. *Earth planet. Sci. Lett.* **14**, 19–25.

LACHENBRUCH, A.H. & SASS, J.H. 1978. Models of an extending lithosphere and heat flow in the Basin and Range province. *In*: SMITH, R.B. & EATON, G.P. (eds) *Cenozoic Tectonics and Regional Geophysics of the Western Cordillera. Mem. geol. Soc. Am.* **152**, 209–50.

LE PICHON, X. 1982. Land-locked oceanic basins and continental collision. *In*: HSU, K. (ed.) *Mountain Building Processes*, pp. 201–11. Academic Press, London.

LOVE, A.E.H. 1911. Some Problems of Geodynamics, pp. 180. Cambridge University Press, Cambridge.

MCKENZIE, D.P. 1972. Active tectonics of the Mediterranean region. *Geophys. J.R. astron. Soc.* **30**, 109–85.

MINSTER, J.B. & JORDAN, T.H. 1984. Vector constraints on Quaternary deformation of the western United States east and west of the San Andreas fault. *In*: CROUCH, J.K. & BACHMAN, S.B. (eds) *Tectonics and Sedimentation along the California Margin. Soc. econ. Paleontol. and Mineral., Pac. sect.*, 1–16.

MOLNAR, P. & CHEN, W.-P. 1983. Focal depths and fault plane solutions of earthquakes under the Tibetan plateau. *J. geophys. Res.* **88**, 1180–96.

—— & TAPPONNIER, P. 1978. Active tectonics of Tibet. *J. geophys. Res.* **83**, 5361–75.

NAVY FLEET NUMERICAL OCEANOGRAPHY CENTER 1982. 10 Minute Elevation Data archived by National Center for Atmospheric Research, Boulder, Colorado, USA.

PARSON, B. & MCKENZIE, D.P. 1978. Mantle convection and the thermal structure of the plates. *J. geophys. Res.* **83**, 4485–96.

PRIESTLEY, K., ORCUTT, J.A. & BRUNE, J.N. 1980. Higher-mode surface waves and structure of the Great basin of Nevada and western Utah. *J. geophys. Res.* **85**, 7166–74.

SMITH, R.B. 1978. Seismicity, crustal structure, and intraplate tectonics of the interior of the western Cordillera. *In*: SMITH, R.B. & EATON, G.P. (eds) *Cenozoic Tectonics and Regional Geophysics of the Western Cordillera. Mem. geol. Soc. Am.* **152**, 111–44.

—— This volume. Kinematics and dynamics of an extending lithosphere: The Basin-Range.

SONDER, L.J. & ENGLAND, P.C. 1986. Vertical averages of rheology of the continental lithosphere: relation to thin sheet parameters. *Earth planet. Sci. Lett.* **77**, 81–90.

—— ,—— & HOUSEMAN, G.A. 1986. Continuum calculations of continental deformation in transcurrent environments. *J. geophys. Res.* **91**, 4797–818.

VILOTTE, J.P., DAIGNIERES, M. & MADARIAGA, R. 1982. Numerical modeling of intraplate deformation: simple mechanical models of continental collision. *J. geophys. Res.* **87**, 10709–28.

WERNICKE, B.P., CHRISTIANSEN, R.L., ENGLAND, P.C. & SONDER, L.J. This volume. Tectonomagmatic evolution of Cenozoic extension in the North American Cordillera.

WYLLIE, P.J. 1977. Crustal anatexis: An experimental review. *Tectonophysics*, **43**, 41–71.

L.J. SONDER*, P.C. ENGLAND†, B.P. WERNICKE & R.L. CHRISTIANSEN††, Department of Geological Sciences, Hoffman Laboratory, Harvard University, Cambridge, MA 02138, USA.

* Present address: Seismological Laboratory, California Institute of Technology, Pasadena, CA 91125, USA.

† Present address: Department of Earth Sciences, Parks Road, Oxford OX1 3PR, UK.

†† Present address: United States Geological Survey, 245 Middlefield Road, Menlo Park, CA 94025, USA.

Appendix

The method used by Houseman & England (1986b) and in this paper adopts the thin-sheet approximation of England & McKenzie (1982, 1983), which amounts to neglecting the stress components τ_{xz} and τ_{yz} (where z is the vertical direction) and letting all other deviatoric stress components represent quantities averaged over the thickness of the lithosphere. We make the further assumption that the deformation is two-dimensional; hence the only non-zero components of the deviatoric stress tensor are the vertically averaged components $\bar{\tau}_{xx}$ and $\bar{\tau}_{zz}$. With the assumption of incompressibility, the horizontal deviatoric stress may be expressed as

$$\bar{\tau}_{xx} = \frac{1}{2L}\left[F_x - \int_{z_t}^{L} \sigma_{zz}\, dz\right], \tag{A1}$$

where L is the thickness of the lithosphere, z_t is the top of the lithosphere, and σ_{zz} equals the lithostatic load. F_x is a constant and may be calculated from the density structure of a reference lithosphere that is in potential energy and isostatic equilibrium with the mid-ocean ridges (see Fig. 3). For isostatically compensated lithosphere columns, differences in $\bar{\tau}_{xx}$ are proportional to differences in their gravitational potential energy (Molnar & Lyon-Caen in prep.).

Once a constitutive relationship is assumed, the horizontal strain rate $\dot{\epsilon}_{xx}$ may be calculated. We use the rheological model of Brace & Kohlstedt (1980), in which the lithosphere deforms by a combination of brittle and ductile mechanisms that depend on temperature, strain rate and depth. For the calculations presented above, we neglect the contribution of the crust to the strength of the lithosphere.

The thermal evolution of the lithosphere is described by

$$\frac{\partial T}{\partial t} + v\frac{\partial T}{\partial z} = \varkappa \frac{\partial^2 T}{\partial z^2} + \frac{H(z)}{\varrho C_p}, \tag{A2}$$

where T is temperature, v is the vertical velocity, $\varkappa$ is thermal diffusivity, H is radiogenic heat production, ϱ is density and C_p is specific heat. We assume that H is constant throughout the crust and is zero in the mantle; $\varkappa$ and C_p are constant everywhere.

The vertical velocity is related to the strain rate by

$$-\dot{\epsilon}_{xx} = \dot{\epsilon}_{zz} = \frac{\partial v}{\partial z}. \tag{A3}$$

We define a measure of extensional strain, β, equal to the ratio of the thickness of crust immediately after compression to that of extended crust. The relationship between β and the horizontal strain rate is

$$\frac{1}{\beta}\frac{\partial \beta}{\partial t} = \dot{\epsilon}_{xx}. \tag{A4}$$

Equations (A2) and (A4) are solved by finite-difference techniques; a Crank–Nicholson scheme is used for (A2) and a modified predictor–corrector scheme is used for (A4). At each time-step $\bar{\tau}_{xx}$ is calculated from the temperature profile and a guess for $\dot{\epsilon}_{xx}$. The value of $\dot{\epsilon}_{xx}$ which gives the correct $\bar{\tau}_{xx}$ (Equation (A1)) is found by iteration using Newton's method.

Boundary and initial conditions

Implicit in the derivation of Equation (A1) is the assumption that shear stresses on the upper and lower surface of the lithosphere are zero. In addition the normal stress σ_{zz} is zero on the upper surface (z_t). For the temperature equation (A2) we assume constant boundary conditions $T = T_0$ and $T = T_1$ on the top and bottom of the lithosphere, respectively.

The initial temperature condition represents the geotherm resulting from instantaneously and uniformly thickening continental lithosphere that is previously in thermal equilibrium with constant heat production, H_0, throughout crust of thickness, h, (see Fig. 3). We assume that all lithosphere below the isotherm T_{MBL} is gravitationally unstable and is replaced by asthenosphere of temperature T_1 at time zero (see text—Description of the Model). Hence the initial temperature condition is

$$\begin{aligned} T &= T_0 + \frac{(T_1 - T_0)z}{fL} + \frac{H_0 L}{2K}\frac{z}{f} \times \left(\frac{2h}{L} - \frac{h^2}{L^2} - \frac{z}{fL}\right) && z \le fh, \\ &= T_0 + \frac{(T_1 - T_0)z}{fL} + \frac{H_0 h^2}{2K}\left(1 - \frac{z}{fL}\right) && fh < z \le z_{\mathrm{BL}}, \\ &= T_1 && z_{\mathrm{BL}} < z, \end{aligned} \tag{A5}$$

where f is the factor by which the lithosphere is thickened, K is thermal conductivity, and z_{BL} is the depth at which the lower part of the lithosphere detaches.